Thermosolutal Marangoni effects on the inclined flow of a binary liquid with variable density. I. Linear stability analysis

J. P. Pascal*
Department of Mathematics, Ryerson University, Toronto, Ontario, M5B 2K3, Canada

S. J. D. D'Alessio†
Department of Applied Mathematics, University of Waterloo, Waterloo, Ontario, N2L 3G1, Canada
(Received 7 July 2016; published 30 December 2016)

We consider the stability of a binary liquid film flowing down a heated incline. A theoretical model is implemented which captures the Soret effect and the dependence of surface tension on both temperature and solutal concentration. The model also allows for variation in the density of the liquid mixture with thermal and solutal differences. A linear stability analysis is performed with asymptotic and numerical results being obtained. The coupling of the effect of a variable density with the thermosolutal-Marangoni instability and the Soret effect is investigated. Good agreement with previous results for the constant density case is found.

DOI: 10.1103/PhysRevFluids.1.083603

I. INTRODUCTION

The founding experiments of Kapitza and Kapitza [1] generated enormous interest in thin films. The onset of instability in inclined thin film flows was first predicted by Benjamin [2] and Yih [3], and the reviews by Craster and Matar [4] and Kalliadasis *et al.* [5] summarize many related studies and findings. Researchers continue to pursue extensions to the original problem investigated by the father-and-son team. Although much progress has been made over the years, new interesting effects continue to emerge as the focus shifts to different aspects associated with the flow. For example, one related aspect concerns the impact of bottom topography on the stability of the flow. The independent studies of D'Alessio *et al.* [6] and Heining and Aksel [7] have shown that, in general, bottom topography tends to stabilize the flow provided that surface tension is not too strong. Another related problem involves variations in surface tension brought on by heating. This gives rise to the thermal Marangoni effect, and the key result here according to the studies of Trevelyan *et al.* [8] and D'Alessio *et al.* [9] is that the thermocapillary effects act to destabilize the flow. Yet another related problem involves the gravity-driven flow down an inclined porous surface. Here Pascal [10] showed that a porous bottom will destabilize the flow when compared to the same flow down an inclined impermeable surface.

Another area of interest regards the role played by surfactants on the stability of gravity-driven flow down an incline. For the case of insoluble surfactants which do not dissolve in the bulk but rather reside on the surface, it was first shown by Benjamin [11] and Whitaker [12] that these surface active agents delay instability when compared to a flow without surfactants. Later investigations include the studies by Blyth and Pozrikidis [13], Pereira *et al.* [14], and Pereira and Kalliadasis [15]. Variations in the surfactant concentration leads to variations in surface tension which in turn gives rise to the solutal Marangoni effect. Karapetsas and Bontozoglou [16,17] recently quantified the stabilizing influence of soluble surfactants. Their results indicate that moderately soluble surfactants may be more effective than insoluble ones.

*jpascal@ryerson.ca
†sdalessio@uwaterloo.ca

In the less studied case of a heated binary liquid film the combined thermal and solutal Marangoni effects may be present as a result of the dependence of surface tension on both the temperature and the concentration of solute. Concentration differences in the liquid are due to a mass flux induced by the temperature gradient. Some of the first investigations involving binary liquids considered a heated horizontal quiescent fluid layer. For example, Bhattacharjee [18] and Joo [19] addressed the stability using constant temperature boundary conditions, while Podolny *et al.* [20–22] and Morozov *et al.* [23] have extensively dealt with the case of a specified heat flux imposed across the fluid layer. In these problems two instability mechanisms may be present: the usual thermocapillarity effect brought on by temperature variations along with the solutocapillarity effect arising from variations in solute concentration. The work by Hu *et al.* [24] was the first to consider the stability of a binary liquid falling down an inclined uniformly heated plate.

The present investigation represents a continuation of the work by Hu *et al.* [24] to also include variations in density. We allow both the density and the surface tension to vary linearly with temperature and solutal concentration. The recent work by D'Alessio *et al.* [25], which examined the impact on stability when several fluid properties are allowed to vary with temperature, has demonstrated that variations in other fluid properties can influence the overall stability of the flow. This research attempts to quantify this influence for the case of a variable density.

This two-part paper is structured as follows. In Sec. II the mathematical formulation of the problem and corresponding boundary conditions are outlined. Following that a linear stability analysis is conducted in Sec. III. Then in Sec. IV we present and discuss our results. The research is summarized in Sec. V. A brief appendix is also included which lists an analytical expression for the critical Reynolds number. Part II is devoted to nonlinear numerical simulations using the weighted residual method and a weakly nonlinear analysis.

II. GOVERNING EQUATIONS

We consider the gravity-driven flow of a thin layer of a binary liquid mixture down an inclined surface. The flow is assumed to remain laminar and two-dimensional with β referring to the angle of inclination with the horizontal. The Cartesian coordinate system (x,z) is oriented with the x axis pointing down the incline and the z axis pointing into the liquid. We denote the velocity components in the x,z directions by u,w, respectively, and the position of the free surface is given by $z = h(x,t)$. The thin liquid layer is heated as a result of the temperature difference, $\Delta T = T_b - T_0$, between the uniformly heated incline and the ambient gas above the liquid where T_b is the temperature of the incline and T_0 is the surrounding gas temperature.

After applying the Boussinesq approximation the governing equations become

$$\frac{\partial u}{\partial x} + \frac{\partial w}{\partial z} = 0, \tag{1}$$

$$\frac{\partial u}{\partial t} + u\frac{\partial u}{\partial x} + w\frac{\partial u}{\partial z} = -\frac{1}{\rho_0}\frac{\partial p}{\partial x} + \frac{g\rho\sin\beta}{\rho_0} + \nu\left(\frac{\partial^2 u}{\partial x^2} + \frac{\partial^2 u}{\partial z^2}\right), \tag{2}$$

$$\frac{\partial w}{\partial t} + u\frac{\partial w}{\partial x} + w\frac{\partial w}{\partial z} = -\frac{1}{\rho_0}\frac{\partial p}{\partial z} - \frac{g\rho\cos\beta}{\rho_0} + \nu\left(\frac{\partial^2 w}{\partial x^2} + \frac{\partial^2 w}{\partial z^2}\right), \tag{3}$$

$$\frac{\partial T}{\partial t} + u\frac{\partial T}{\partial x} + w\frac{\partial T}{\partial z} = \kappa\left(\frac{\partial^2 T}{\partial x^2} + \frac{\partial^2 T}{\partial z^2}\right), \tag{4}$$

$$\frac{\partial C}{\partial t} + u\frac{\partial C}{\partial x} + w\frac{\partial C}{\partial z} = D_m\left[\frac{\partial^2 C}{\partial x^2} + \frac{\partial^2 C}{\partial z^2} + \chi\left(\frac{\partial^2 T}{\partial x^2} + \frac{\partial^2 T}{\partial z^2}\right)\right], \tag{5}$$

where p is the pressure, T is the temperature, C is the solutal concentration, g is the acceleration due to gravity, ν is the kinematic viscosity, ρ is the variable mass density with ρ_0 denoting a reference value, κ is the thermal diffusivity, D_m is the mass diffusivity, and χ is the Soret coefficient. We note that the contribution to the solutal concentration brought on by temperature variations is known as the Soret effect and is measured by the parameter χ. Following Hu *et al.* [24] we have ignored the Dufour effect, which accounts for changes in temperature resulting from changes in solutal concentration.

We will allow the surface tension to vary linearly with temperature and solutal concentration according to

$$\sigma = \sigma_0 - \gamma_T(T - T_0) + \gamma_C(C - C_0),$$

where σ is the surface tension and σ_0, T_0, C_0 represent reference values of σ, T, C, respectively. We will assume that surface tension decreases with temperature, but increases with concentration, so the rate of change parameters γ_T and γ_C will be assigned nonnegative values.

For the variable fluid density we again assume a linear dependence on temperature and solutal concentration of the form

$$\frac{\rho}{\rho_0} = 1 - \hat{\alpha}_T(T - T_0) - \hat{\alpha}_C(C - C_0),$$

where ρ_0 denotes the reference density attained at $T = T_0$ and $C = C_0$, and $\hat{\alpha}_T$ and $\hat{\alpha}_C$ are the thermal and solutal expansion coefficients. This formulation for the density has been employed by Hu *et al.* [26] to study the stability of Poiseuille-Rayleigh-Benard flows exhibiting the Soret effect. The parameter $\hat{\alpha}_T$ is taken to be nonnegative, and as such the fluid is assumed to expand if heated. On the other hand, $\hat{\alpha}_C$ can take on negative and nonnegative values, which will thus include cases of decrease and increase in density with solutal concentration.

The other fluid properties are, as in Ref. [26], assumed to remain constant. Some of these, such as viscosity, can vary with temperature, but it is only density and surface tension that will realistically depend on both temperature and concentration, and we expect this combined variation to be more relevant in connection with the Soret effect.

The system of equations (1)–(5) is to be solved subject to the following conditions. Along the free surface $z = h(x,t)$ we apply the dynamic boundary conditions

$$p = p_0 + \frac{2\mu}{F}\left(\left[\frac{\partial h}{\partial x}\right]^2 \frac{\partial u}{\partial x} + \frac{\partial w}{\partial z} - \frac{\partial h}{\partial x}\left[\frac{\partial u}{\partial z} + \frac{\partial w}{\partial x}\right]\right) - \frac{\sigma}{F^{3/2}}\frac{\partial^2 h}{\partial x^2}, \tag{6}$$

$$\sqrt{F}\left(\frac{\partial \sigma}{\partial x} + \frac{\partial h}{\partial x}\frac{\partial \sigma}{\partial z}\right) = \mu\left[G\left(\frac{\partial u}{\partial z} + \frac{\partial w}{\partial x}\right) - 4\frac{\partial h}{\partial x}\frac{\partial u}{\partial x}\right], \tag{7}$$

where

$$F = 1 + \left[\frac{\partial h}{\partial x}\right]^2, \quad G = 1 - \left[\frac{\partial h}{\partial x}\right]^2,$$

the kinematic condition which in the absence of evaporation leads to

$$w = \frac{\partial h}{\partial t} + u\frac{\partial h}{\partial x}, \tag{8}$$

Newton's law of cooling

$$-\alpha_g\sqrt{F}(T - T_0) = \lambda\left(\frac{\partial T}{\partial z} - \frac{\partial h}{\partial x}\frac{\partial T}{\partial x}\right), \tag{9}$$

and the zero mass flux condition

$$\frac{\partial C}{\partial z} - \frac{\partial h}{\partial x}\frac{\partial C}{\partial x} + \chi\left(\frac{\partial T}{\partial z} - \frac{\partial h}{\partial x}\frac{\partial T}{\partial x}\right) = 0. \tag{10}$$

In the above p_0 refers to the pressure in the ambient gas, μ is the dynamic viscosity, α_g is the heat transfer coefficient, and λ is the thermal conductivity. The dynamic conditions (6) and (7) are based on the assumption that the ambient gas is dynamically passive. Condition (6) represents the balance between the normal force exerted by the flow, surface tension, and the ambient pressure, while condition (7) equates the tangential stress due to the flow to the Marangoni stress resulting from the variation in surface tension. At the bottom $z = 0$ we apply the no-slip, impermeability, zero mass flux, and constant temperature conditions given by

$$u = w = \frac{\partial C}{\partial z} + \chi \frac{\partial T}{\partial z} = 0, \quad T = T_b. \tag{11}$$

We next render the equations in dimensionless form by choosing the Nusselt thickness, H, given by

$$H = \left(\frac{3\mu Q}{g\rho_0 \sin\beta} \right)^{1/3},$$

to be the length scale where Q denotes the constant volume flux. The velocity scale is $U = Q/H$ while the time scale is H/U. The scaled pressure, temperature, and concentration, denoted by an asterisk, are

$$p = p_0 + \rho_0 U^2 p^*, \quad C = C_0 + \frac{\gamma_T \Delta T}{\gamma_C} C^*, \quad T = T_0 + (\Delta T) T^*,$$

respectively. The dimensionless equations, with the asterisk removed for notational convenience, become

$$\frac{\partial u}{\partial x} + \frac{\partial w}{\partial z} = 0, \tag{12}$$

$$\mathrm{Re}\left(\frac{\partial u}{\partial t} + u\frac{\partial u}{\partial x} + w\frac{\partial u}{\partial z} \right) = -\mathrm{Re}\frac{\partial p}{\partial x} + 3(1 - \alpha_T T - \alpha_C C) + \frac{\partial^2 u}{\partial x^2} + \frac{\partial^2 u}{\partial z^2}, \tag{13}$$

$$\mathrm{Re}\left(\frac{\partial w}{\partial t} + u\frac{\partial w}{\partial x} + w\frac{\partial w}{\partial z} \right) = -\mathrm{Re}\frac{\partial p}{\partial z} - 3\cot\beta(1 - \alpha_T T - \alpha_C C) + \frac{\partial^2 w}{\partial x^2} + \frac{\partial^2 w}{\partial z^2}, \tag{14}$$

$$\mathrm{Pr}\,\mathrm{Re}\left(\frac{\partial T}{\partial t} + u\frac{\partial T}{\partial x} + w\frac{\partial T}{\partial z} \right) = \frac{\partial^2 T}{\partial x^2} + \frac{\partial^2 T}{\partial z^2}, \tag{15}$$

$$\mathrm{Sc}\,\mathrm{Re}\left(\frac{\partial C}{\partial t} + u\frac{\partial C}{\partial x} + w\frac{\partial C}{\partial z} \right) = \frac{\partial^2 C}{\partial x^2} + \frac{\partial^2 C}{\partial z^2} + \mathrm{So}\left(\frac{\partial^2 T}{\partial x^2} + \frac{\partial^2 T}{\partial z^2} \right), \tag{16}$$

where $\mathrm{Re} = Q/\nu$ is the Reynolds number, $\mathrm{Pr} = \nu/\kappa$ is the Prandtl number, $\mathrm{Sc} = \nu/D_m$ is the Schmidt number, $\mathrm{So} = \chi\gamma_c/\gamma_T$ is the Soret number, and $\alpha_T = \hat{\alpha}_T \Delta T, \alpha_C = \hat{\alpha}_C \gamma_T \Delta T/\gamma_C$ are the dimensionless thermal and solutal expansion coefficients, respectively.

The corresponding dimensionless free-surface conditions along $z = h(x,t)$ become

$$p = \frac{2}{\mathrm{Re}F}\left(\left[\frac{\partial h}{\partial x}\right]^2 \frac{\partial u}{\partial x} + \frac{\partial w}{\partial z} - \frac{\partial h}{\partial x}\left[\frac{\partial u}{\partial z} + \frac{\partial w}{\partial x} \right] \right) - \frac{[\mathrm{We} - M(T - C)]}{F^{3/2}} \frac{\partial^2 h}{\partial x^2}, \tag{17}$$

$$-M\mathrm{Re}\sqrt{F}\left[\frac{\partial}{\partial x}(T - C) + \frac{\partial h}{\partial x}\frac{\partial}{\partial z}(T - C) \right] = G\left(\frac{\partial u}{\partial z} + \frac{\partial w}{\partial x} \right) - 4\frac{\partial h}{\partial x}\frac{\partial u}{\partial x}, \tag{18}$$

$$w = \frac{\partial h}{\partial t} + u\frac{\partial h}{\partial x}, \tag{19}$$

$$-B\sqrt{F}T = \frac{\partial T}{\partial z} - \frac{\partial h}{\partial x}\frac{\partial T}{\partial x}, \tag{20}$$

$$\frac{\partial C}{\partial z} - \frac{\partial h}{\partial x}\frac{\partial C}{\partial x} + So\left(\frac{\partial T}{\partial z} - \frac{\partial h}{\partial x}\frac{\partial T}{\partial x} \right) = 0, \tag{21}$$

where $\mathrm{We} = \sigma_0/(\rho_0 H U^2)$ is the Weber number, $M = \gamma_T \Delta T/(\rho_0 H U^2)$ is the scaled gradient of surface tension with respect to temperature, and $B = \alpha_g H/\lambda$ is the scaled heat transfer coefficient.

Finally, the dimensionless bottom conditions at $z = 0$ become

$$u = w = \frac{\partial C}{\partial z} + \mathrm{So}\frac{\partial T}{\partial z} = 0, \quad T = 1. \tag{22}$$

III. STABILITY ANALYSIS

We begin by determining the steady flow possessing no variations in the x direction. If we denote this steady flow by $T = T_s(z), C = C_s(z), p = p_s(z)$, $u = u_s(z), w = w_s(z) = 0$ and $h_s = 1$ it is a straight-forward exercise to deduce that

$$\begin{aligned}
T_s(z) &= 1 - \frac{B}{1+B}z,\\
C_s(z) &= \frac{B\mathrm{So}}{1+B}z,\\
p_s(z) &= -\frac{3\cot\beta}{\mathrm{Re}}\left[(1-\alpha_T)(z-1) + \frac{B_1}{2}(z^2-1)\right],\\
u_s(z) &= -\frac{B_1}{2}z^3 - \frac{3}{2}(1-\alpha_T)z^2 + C_1 z,
\end{aligned}$$

where

$$B_1 = \frac{B(\alpha_T - \alpha_C\mathrm{So})}{1+B}, \quad C_1 = 3(1-\alpha_T) + \frac{3}{2}B_1,$$

and without loss of generality we set $C_s(0) = 0$. It is worth noting the departure from the linear hydrostatic pressure and parabolic velocity profile as a result of the variable density. The constant density case can be easily recovered by setting $\alpha_T = \alpha_C = 0$. We also point out the limiting cases: $B = 0$ corresponding to an insulated fluid layer having the constant temperature $T_s(z) = 1$, and $B \to \infty$ corresponding to an infinite rate of heat transfer across the interface giving rise to the temperature profile $T_s(z) = 1 - z$.

To investigate the stability we superimpose infinitesimal disturbances on the steady flow and then monitor how the disturbances evolve in time. The perturbed flow is expressed as

$$\begin{aligned}
u &= u_s(z) + \tilde{u}(x,z,t), \quad w = \tilde{w}(x,z,t), \quad p = p_s(z) + \tilde{p}(x,z,t),\\
T &= T_s(z) + \tilde{T}(x,z,t), \quad C = C_s(z) + \tilde{C}(x,z,t), \quad h = 1 + \eta(x,t),
\end{aligned}$$

where η is the imposed perturbation in the fluid thickness while the tilde denotes perturbations in the other quantities. We linearize the problem with respect to the disturbances and introduce normal modes

$$(\tilde{u},\tilde{w},\tilde{p},\tilde{T},\tilde{C},\eta) = (\hat{u}(z),\hat{w}(z),\hat{p}(z),\hat{T}(z),\hat{C}(z),\hat{\eta})e^{ik(x-ct)}.$$

The wave number k is taken to be real and positive, while c is a complex quantity where the real part is the phase speed and the imaginary part, denoted by $\mathrm{Im}(c)$, is related to the growth rate. We obtain the following equations for the z-dependent factors

$$D\hat{w} + ik\hat{u} = 0, \tag{23}$$

$$\mathrm{Re}[ik(u_s - c)\hat{u} + (Du_s)\hat{w}] = -ik\mathrm{Re}\hat{p} - 3(\alpha_T\hat{T} + \alpha_C\hat{C}) + D^2\hat{u} - k^2\hat{u}, \tag{24}$$

$$ik\mathrm{Re}(u_s - c)\hat{w} = -\mathrm{Re}D\hat{p} + 3\cot\beta(\alpha_T\hat{T} + \alpha_C\hat{C}) + D^2\hat{w} - k^2\hat{w}, \tag{25}$$

$$\mathrm{Pr}\,\mathrm{Re}[ik(u_s - c)\hat{T} + (DT_s)\hat{w}] = D^2\hat{T} - k^2\hat{T}, \tag{26}$$

$$\mathrm{Sc}\,\mathrm{Re}[ik(u_s - c)\hat{C} + (DC_s)\hat{w}] = D^2\hat{C} - k^2\hat{C} + \mathrm{So}(D^2\hat{T} - k^2\hat{T}). \tag{27}$$

Here D denotes the differential operator $D \equiv d/dz$. Transferring the boundary conditions at $z = 1 + \eta$ to $z = 1$ and linearizing yields the following free-surface conditions at $z = 1$:

$$\hat{p} = \frac{3B_2 \cot\beta}{\mathrm{Re}}\hat{\eta} + \frac{2}{\mathrm{Re}}D\hat{w} + k^2\{\mathrm{We} - M[T_s(1) - C_s(1)]\}\hat{\eta}, \tag{28}$$

$$-ikM\mathrm{Re}\{\hat{T} - \hat{C} + [DT_s(1) - DC_s(1)]\hat{\eta}\} = [D^2u_s(1)]\hat{\eta} + D\hat{u} + ik\hat{w}, \tag{29}$$

$$\hat{w} = ik[u_s(1) - c]\hat{\eta}, \tag{30}$$

$$D\hat{T} + B\hat{T} + B[DT_s(1)]\hat{\eta} = 0, \tag{31}$$

$$D\hat{C} + \mathrm{So}D\hat{T} = 0, \tag{32}$$

where

$$B_2 = \frac{1 - \alpha_T + B(1 - \alpha_C\mathrm{So})}{1 + B}.$$

At $z = 0$ we have

$$\hat{u} = \hat{w} = \hat{T} = D\hat{C} + \mathrm{So}D\hat{T} = 0. \tag{33}$$

By combining Eqs. (24)–(25) the pressure can be eliminated. If we also introduce the perturbed stream function defined as

$$\tilde{u}(x,z,t) = \frac{\partial\psi}{\partial z}, \quad \tilde{w}(x,z,t) = -\frac{\partial\psi}{\partial x},$$

and set $\psi(x,z,t) = \phi(z)e^{ik(x-ct)}$, then the system of equations (23)–(27) simplifies to

$$\begin{aligned} &D^4\phi - [ik\mathrm{Re}(u_s - c) + 2k^2]D^2\phi + [ik^3\mathrm{Re}(u_s - c) + k^4 + ik\mathrm{Re}D^2u_s]\phi \\ &\quad = 3ik\cot\beta(\alpha_T\hat{T} + \alpha_C\hat{C}) + 3(\alpha_T D\hat{T} + \alpha_C D\hat{C}), \end{aligned} \tag{34}$$

$$\mathrm{Pr}\,\mathrm{Re}[ik(u_s - c)\hat{T} - ik(DT_s)\phi] = D^2\hat{T} - k^2\hat{T}, \tag{35}$$

$$\mathrm{Sc}\,\mathrm{Re}[ik(u_s - c)\hat{C} - ik(DC_s)\phi] = D^2\hat{C} - k^2\hat{C} + \mathrm{So}(D^2\hat{T} - k^2\hat{T}). \tag{36}$$

The boundary conditions at $z = 1$ transform to

$$\begin{aligned} &D^3\phi - [ik\mathrm{Re}(u_s(1) - c) + 3k^2]D\phi \\ &\quad = 3(\alpha_T\hat{T} + \alpha_C\hat{C}) + (3ikB_2\cot\beta + ik^3\mathrm{Re}\{\mathrm{We} - M[T_s(1) - C_s(1)]\})\hat{\eta}, \end{aligned} \tag{37}$$

$$D^2\phi + k^2\phi + ikM\mathrm{Re}(\hat{T} - \hat{C}) + \{D^2u_s(1) + ikM\mathrm{Re}[DT_s(1) - DC_s(1)]\}\hat{\eta} = 0, \tag{38}$$

$$\phi + [u_s(1) - c]\hat{\eta} = 0, \tag{39}$$

$$D\hat{T} + B\hat{T} + B[DT_s(1)]\hat{\eta} = 0, \tag{40}$$

$$D\hat{C} + \mathrm{So}D\hat{T} = 0, \tag{41}$$

while the bottom conditions at $z = 0$ become

$$\phi = D\phi = \hat{T} = D\hat{C} + \mathrm{So}D\hat{T} = 0. \tag{42}$$

The system of equations (34)–(42) is posed as an eigenvalue problem where c denotes the eigenvalue. We begin by carrying out an asymptotic analysis for small wave numbers by letting $k \to 0$ and expanding the perturbations in powers of k as follows:

$$\begin{aligned}
\phi &= \phi_0(z) + ik\phi_1(z) + O(k^2),\\
\hat{C} &= \hat{C}_0(z) + ik\hat{C}_1(z) - k^2\hat{C}_2(z) + O(k^3),\\
\hat{T} &= \hat{T}_0(z) + ik\hat{T}_1(z) - k^2\hat{T}_2(z) + O(k^3),\\
\hat{\eta} &= \hat{\eta}_0 + ik\hat{\eta}_1 + O(k^2).
\end{aligned}$$

The eigenvalue is similarly expanded as

$$c = c_0 + ikc_1 + O(k^2).$$

With this formulation for the expansions, the undetermined quantities will be real, and consequently the growth rate is given by k^2c_1, with neutral stability occurring when $c_1 = 0$. When the above are substituted into (34)–(42) and all parameters are assumed to be $O(1)$ as $k \to 0$, we obtain a hierarchy of problems at various orders of k. In solving these problems we find that $\hat{\eta}_0$ is arbitrary, and the neutral stability relation is independent of $\hat{\eta}_1$. Thus, without loss of generality we set $\hat{\eta}_0 = 1$ and $\hat{\eta}_1 = 0$ in the analysis that follows.

The leading-order problem satisfies

$$D^4\phi_0 = 3\alpha_T D\hat{T}_0 + 3\alpha_C D\hat{C}_0, \tag{43}$$

$$D^2\hat{T}_0 = 0, \tag{44}$$

$$D^2\hat{C}_0 = 0, \tag{45}$$

subject to

$$\phi_0(0) = D\phi_0(0) = 0, \tag{46}$$

$$D^3\phi_0(1) - 3\alpha_T\hat{T}_0(1) - 3\alpha_C\hat{C}_0(1) = 0, \tag{47}$$

$$D^2\phi_0(1) + D^2u_s(1) = 0, \tag{48}$$

$$\phi_0(1) + u_s(1) - c_0 = 0, \tag{49}$$

$$\hat{T}_0(0) = 0, \quad D\hat{T}_0(1) + B\hat{T}_0(1) - \frac{B^2}{1+B} = 0, \tag{50}$$

$$D\hat{C}_0(0) + \mathrm{So}\hat{T}_0(0) = D\hat{C}_0(1) + \mathrm{So}\hat{T}_0(1) = 0. \tag{51}$$

The solution to this system is given by

$$\begin{aligned}
\phi_0(z) &= B^2(\alpha_T - \alpha_C\mathrm{So})z^4 + 4\,(B+1)^2z^2\alpha_C(z-3)\hat{C}_{00} - [6\,(3\,B^2 + 4\,B + 2)\alpha_T\\
&\quad - 6\,\alpha_C\mathrm{So}\,B^2 - 12\,(B+1)^2(1+B_1)]z^2,\\
\hat{T}_0(z) &= \frac{2B^2}{3(1+B)^2}z,\\
\hat{C}_0(z) &= -\frac{2B^2\mathrm{So}}{3(1+B)^2}z + \hat{C}_{00},\\
c_0 &= 3 - \alpha_C\hat{C}_{00} - \frac{(9\,B^2 + 28\,B + 24)\alpha_T}{8(B+1)^2} - \frac{5B\mathrm{So}\,(3\,B+4)\alpha_C}{8(B+1)^2},
\end{aligned} \tag{52}$$

where the constant $\hat{C}_{00}$ can be determined from the $O(k)$ problem.

At $O(k)$ Eq. (36) and conditions (41) and (42) yield

$$\mathrm{Sc}\,\mathrm{Re}[(u_s - c_0)\hat{C}_0 - DC_s\phi_0] = D^2\hat{C}_1 + \mathrm{So}D^2\hat{T}_1,$$

subject to the conditions

$$D\hat{C}_1 + \mathrm{So}D\hat{T}_1 = 0 \quad \text{at} \quad z = 0,1. \tag{53}$$

Solving the differential equation for $D\hat{C}_1 + \mathrm{So}D\hat{T}_1$ and substituting into the conditions, we find that we must have

$$\hat{C}_{00} = \frac{\mathrm{So}[(9\mathrm{So}\alpha_C - 20c_0 - 54\alpha_T + 36B_1 + 45)B^3 - (20c_0 + 65\alpha_T - 56B_1 - 65)B^2 + (20\alpha_T - 20B_1 - 20)B]}{5(3B\mathrm{So}\alpha_C - 8Bc_0 - 8B\alpha_T + 5BB_1 + 8B - 8c_0 - 8\alpha_T + 5B_1 + 8)(B+1)^2}.$$

From the $O(k)$ problem we also obtain

$$\mathrm{Pr}\,\mathrm{Re}[(u_s - c_0)\hat{T}_0 - DT_s\phi_0] = D^2\hat{T}_1,$$

subject to the conditions

$$D\hat{T}_1(1) + B\hat{T}_1(1) = 0 \quad \text{and} \quad \hat{T}_1(0) = 0. \tag{54}$$

From the above we can determine $\hat{T}_1$, and then obtain the solution for $\hat{C}_1$ to within an additive constant $\hat{C}_{10}$. This constant is determined in a similar manner to $\hat{C}_{00}$ by using the $O(k^2)$ terms in the concentration equation and the mass flux conditions given by

$$\mathrm{Sc}\,\mathrm{Re}[(u_s - c_0)\hat{C}_1 - c_1\hat{C}_0 - DC_s\phi_1] = D^2\hat{C}_2 + \mathrm{So}D^2\hat{T}_2 + \hat{C}_0 + \mathrm{So}\hat{T}_0$$

and

$$D\hat{C}_2 + \mathrm{So}D\hat{T}_2 = 0 \quad \text{at} \quad z = 0,1. \tag{55}$$

From the $O(k)$ terms we can then construct the following problem for ϕ_1:

$$D^4\phi_1 - \mathrm{Re}(u_s - c_0)D^2\phi_0 + \mathrm{Re}D^2u_s\phi_0 - 3\alpha_T D\hat{T}_1 - 3\alpha_C D\hat{C}_1 - 3\cot\beta(\alpha_T\hat{T}_0 + \alpha_C\hat{C}_0) = 0,$$

$$D^3\phi_1(1) - \mathrm{Re}[u_s(1) - c_0]D\phi_0(1) - 3\alpha_T\hat{T}_1(1) - 3\alpha\hat{C}_1(1) - 3\cot\beta B_2 = 0, \tag{56}$$

$$D^2\phi_1(1) + M\mathrm{Re}[\hat{T}_0(1) - \hat{C}_0(1) + DT_s(1) - DC_s(1)] = 0, \tag{57}$$

$$\phi_1(0) = D\phi_1(0) = 0. \tag{58}$$

We obtained explicit solutions for $\hat{C}_1$, $\hat{T}_1$, and ϕ_1 using the Maple symbolic algebra software; however, the expressions are very long, and presenting them would not serve a useful purpose.

The $O(k)$ terms in the kinematic condition give $\phi_1(1) = 0$, and letting $c_1 = 0$ in this equation gives the state of neutral stability. We solved this for Re using Maple and obtained an expression for the critical Reynolds number in terms of the other parameters of the problem. The expression is too long to list in its entirety, so in the Appendix we present its asymptotic approximation for small values of the density variation parameters.

For the constant density case our expression reduces to

$$\mathrm{Re}_{\mathrm{crit}} = \frac{10(1+B)^2\cot\beta}{12(1+B)^2 + \frac{5}{16}MB(16 + 12\mathrm{So} + 3\mathrm{So}B)}, \tag{59}$$

which is in full agreement with the result obtained by Hu *et al.* [24] once we correct for the change in scales. Further disregarding the Soret effect by setting $\mathrm{So} = 0$ we obtain the expression obtain by D'Alessio *et al.* [9] which accounts for thermocapillary effects. If the thermal effects are completely disregarded by also setting $M = 0$ the well-known isothermal result is obtained: $\mathrm{Re}_{\mathrm{crit}} = 5\cot\beta/6$. We can conclude that the obtained result for $\mathrm{Re}_{\mathrm{crit}}$ corresponds to the onset of inertial instability, referred to as the H mode, enhanced by thermocapillary and solutocapillary effects.

It is evident that the expression for the critical Reynolds number give by Eq. (59) is a decreasing function of So, and hence increasing the Soret number destabilizes the flow. We also point out that if $B = 0$ this expression reproduces the expected isothermal result while in the limit $B \to \infty$ we obtain

$$\mathrm{Re}_{\mathrm{crit}} \to \frac{10\cot\beta}{12 + \frac{15}{16} M\mathrm{So}}.$$

As B is increased from zero a minimum critical Reynolds number, $\mathrm{Re}_{\mathrm{crit,min}}$, is attained when $B = (8 + 6\mathrm{So})/(8 + 3\mathrm{So})$ and is given by

$$\mathrm{Re}_{\mathrm{crit,min}} = \frac{10\cot\beta}{12 + \frac{5M(4+3\mathrm{So})^2}{4(16+9\mathrm{So})}}.$$

This dependence on B can be explained as follows. When $B = 0$ the steady-state temperature within the fluid layer is constant while the concentration is zero; thus, the free-surface temperature and concentration are uniform, which neutralizes the thermosolutocapillary effects. As B is increased a variation in free-surface temperature and concentration develops which triggers the thermal and solutal Marangoni effects. However, for large B the temperature along the free surface approaches that of the constant ambient medium while the concentration approaches So, and as such the thermal and solutal Marangoni effects are again weakened. Consequently, there exists an optimal value of B for which these effects are maximized resulting in a minimum value for $\mathrm{Re}_{\mathrm{crit}}$. Last, $\mathrm{Re}_{\mathrm{crit}}$ does not depend on the parameters Pr, Sc, and We.

IV. RESULTS AND DISCUSSION

It is well known that the Marangoni effect can even occur in stationary fluid layers with nondeformable surfaces [5]. In these cases perturbations in temperature and concentration along the surface cause variations in surface tension which induces flow along the surface. The resulting long-wave instability is referred to as the S mode, while instability of short perturbations of length comparable to the thickness of the fluid layer is referred to as the P mode [5]. In order for the analysis to capture these other modes we must consider the implicit dependence of the parameters We, M, and B on the Reynolds number. To this end we introduce the new parameters Ka, Ma, and Bi by letting

$$\mathrm{We} = \left(\frac{3}{\sin\beta}\right)^{1/3} \frac{\mathrm{Ka}}{\mathrm{Re}^{5/3}}, \quad M = \left(\frac{3}{\sin\beta}\right)^{1/3} \frac{\mathrm{Ma}}{\mathrm{Re}^{5/3}}, \quad B = \left(\frac{3}{\sin\beta}\right)^{1/3} \mathrm{Bi}\,\mathrm{Re}^{1/3},$$

where

$$\mathrm{Ka} = \frac{\sigma_0 \rho_0^{1/3}}{g\mu^{4/3}} \text{ is the Kapitza number,}$$

$$\mathrm{Ma} = \frac{\gamma_T \Delta T \rho_0^{1/3}}{g\mu^{4/3}} \text{ is the Marangoni number, and}$$

$$\mathrm{Bi} = \frac{\alpha_g \mu^{2/3}}{g\lambda\rho_0^{2/3}} \text{ is the Biot number.}$$

In terms of these new parameters the neutral stability obtained from the asymptotic analysis, can, depending on the value of the parameters, have two solutions for the Reynolds number. These values indicate the onset of instability of the S and H modes.

It should be pointed out that the asymptotic analysis can only predict the instability of very long perturbations. To determine the stability of perturbations in general we must resort to numerical solutions of the eigenvalue problem. We used a Chebyshev spectral collocation method to calculate the eigenvalues of the problem (34)–(42). Shown in Figs. 1–3 are neutral stability curves in the Re-k plane. The intercepts of these curves with the Reynolds number axis correspond to the critical

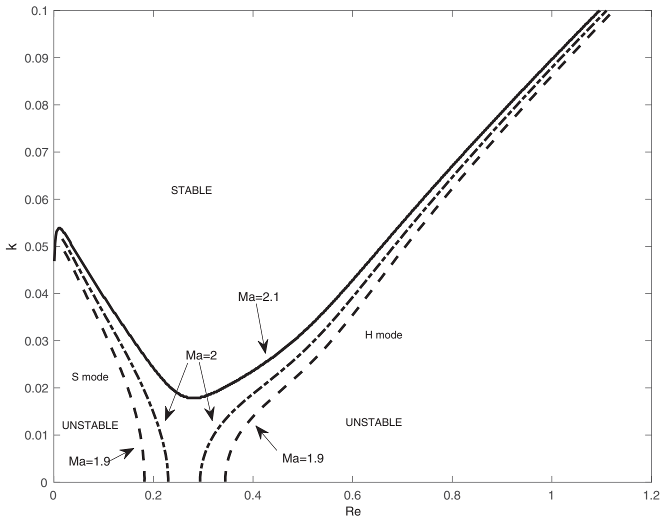

FIG. 1. Neutral stability curves for various Ma values with So $= -0.5$, $\alpha_T = 0.2$, $\alpha_C = 0.2$, Pr $= 7$, Sc $= 700$, Ka $= 100$, Bi $= 1$, and $\cot\beta = 1$.

Reynolds number for the onset of instability of perturbations with $k = 0$. These values are in excellent agreement with the formula from the asymptotic analysis for parameter values that are $O(1)$.

Before we interpret our results we discuss the numerical restrictions and realistic ranges for the parameters. Now, in terms of scaled quantities the density is given by

$$\mathcal{P} \equiv \frac{\rho}{\rho_0} = 1 - \alpha_T T - \alpha_C C.$$

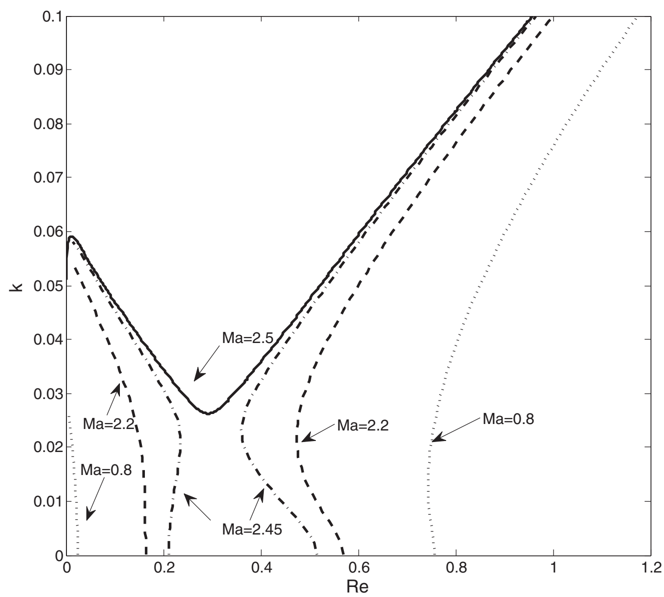

FIG. 2. Neutral stability curves for various Ma values with So $= -0.5$, $\alpha_T = 0$, $\alpha_C = 0$, Pr $= 7$, Sc $= 700$, Ka $= 100$, Bi $= 1$, and $\cot\beta = 1$.

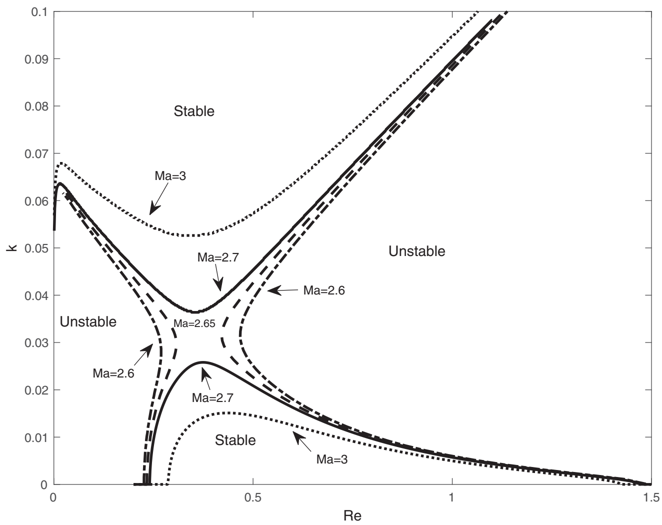

FIG. 3. Neutral stability curves for various Ma values with $\mathrm{So} = -0.5$, $\alpha_T = 0.2$, $\alpha_C = -0.2$, $\mathrm{Pr} = 7$, $\mathrm{Sc} = 700$, $\mathrm{Ka} = 100$, $\mathrm{Bi} = 1$, and $\cot\beta = 1$.

Consequently then, for the equilibrium flow the density distribution is

$$\mathcal{P}_s(z) = 1 - \alpha_T + (\alpha_T - \alpha_C \mathrm{So})\frac{B}{B+1}z, \quad 0 \leqslant z \leqslant 1. \tag{60}$$

It is evident from this expression that the density will attain negative values if $\alpha_T \geqslant 1$, so α_T will be restricted to nonnegative values less than 1. Now, if in addition the values of α_C and So have the opposite sign or one of them is zero, then the density is positive throughout the equilibrium flow. If these two parameters have the same sign, the density will be a positive function of z for all values of B as long as $\alpha_C \mathrm{So} < 1$. However, since we are approximating the density by a linear approximation, we should restrict α_C to absolute values less than 1. In this case the density will be positive if $|\mathrm{So}| < 1$. This includes the range of Soret numbers considered by Hu *et al.* [24]. We point out the special case when $\alpha_T = \alpha_C \mathrm{So}$. Here at equilibrium the density will be uniform throughout the liquid layer.

In order to determine realistic ranges for our thermal and solutal expansion coefficients, we make comparisons with the parameter values employed by Hu *et al.* [26] in their study of convective instability in Poiseuille flow. They considered cases consistent with binary liquids such as ethanol-water mixtures. The relevant parameters in their investigation are the Rayleigh number and the separation factor, which in terms of our scaling are expressed as

$$\mathrm{Ra} = 3\alpha_T \mathrm{Pr}\,\mathrm{Re}\cot\beta$$

and

$$\Psi = -\frac{\alpha_C}{\alpha_T}\mathrm{So},$$

respectively. In our investigation we have set $\cot\beta = 1$ and $\mathrm{Pr} = 7$ and considered Reynolds numbers less than 2. Therefore, with α_T restricted to values less than 1 as described above, we are considering Rayleigh numbers ranging up to approximately 40. These values are insufficient for generating outright Benard-Rayleigh instability; however, our aim in this study is to investigate how a variable density couples with the various instability mechanisms affecting inclined free surface flows. Regarding the separation factor, Hu *et al.* [26] have considered values in the range $|\Psi| \leqslant 0.5$. The cases examined in our investigation fall within this range. Finally, in our investigation we set

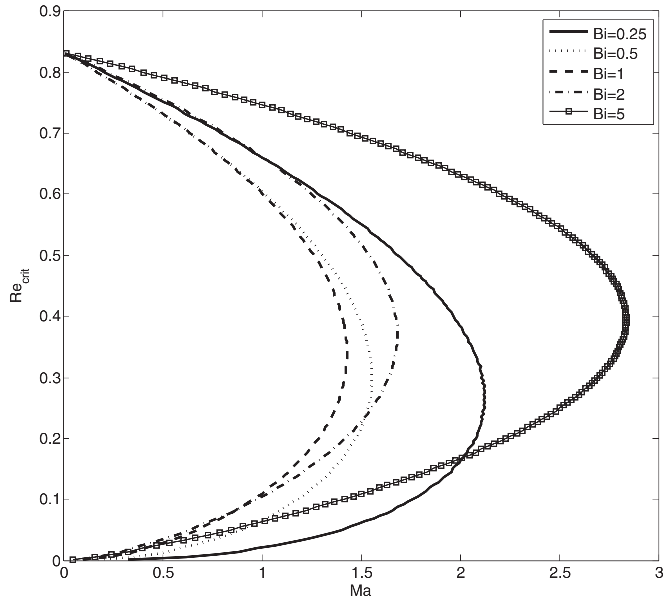

FIG. 4. $\mathrm{Re}_{\mathrm{crit}}$ vs Ma for various Bi values with $\mathrm{Pr} = 7$, $\mathrm{Ka} = 100$, $\alpha_T = \alpha_C = \mathrm{So} = 0$, and $\cot\beta = 1$.

the value of the Schmidt number to $\mathrm{Sc} = 700$, which corresponds to a value of 0.01 for the Lewis number, $\mathrm{Le} = \mathrm{Pr}/\mathrm{Sc}$, as was used in Ref. [24,26].

The results in Fig. 1 show that as the Marangoni number increases, both the S and H modes are destabilized, and the two eventually merge corresponding to an equilibrium flow that is unstable for all Reynolds numbers. It is also apparent that the onset of instability for both modes is due to the amplification of the infinitely long perturbations. These general aspects are the same as those observed for the basic nonisothermal problem [5] and the basic thermosolutal problem with nonnegative values for the Soret number as presented by Hu *et al.* [24]. However, as is illustrated in Fig. 2, our results reveal that if the Soret number is negative and of sufficiently large absolute value, then, if the Marangoni number is large enough, the neutral stability curves for the S and H modes exhibit a "nose-like" profile. More specifically, the onset of instability in the equilibrium flow is not the result of the instability of infinitely long perturbations, but rather the amplification of perturbations of finite wavelength. Regarding the effect of a variable density on this phenomenon, it turns out that the variation with concentration parameter, α_C has an important qualitative and quantitative effect. We find that if α_C is positive and sufficiently large, as is the case in Fig. 1, then the phenomenon is suppressed. However, as is exemplified in Fig. 3, if the Soret number and α_C have the same sign, and if their product is sufficiently large, then the effect on the H-mode branch is greatly amplified, i.e., there is a larger difference between the critical Reynolds number for the onset of instability of the equilibrium flow and that for the instability of perturbations with $k = 0$.

Of particular interest is to investigate the effect of the parameters of the problem on the interval of Reynolds numbers for which the equilibrium flow is stable. To accomplish this we analyze the critical Reynolds number for the onset of the S and H modes as a function of Ma for different values of the other parameters. In Fig. 4 we have $\mathrm{Re}_{\mathrm{crit}}$ versus Ma for various Bi values. The upper branch of the curve corresponds to the onset of instability of the H mode, while the lower branch corresponds to the S mode. The region inside the curve measures the interval of Reynolds numbers for which the flow is stable. As discussed above, as Bi is increased from zero the extent of the region of stability decreases, attains a minimum and then increases. Additional information provided by these results is that the H and S modes both experience the destabilizing effect with Bi for smaller values of Bi and a stabilizing effect with Bi if these values are sufficiently large.

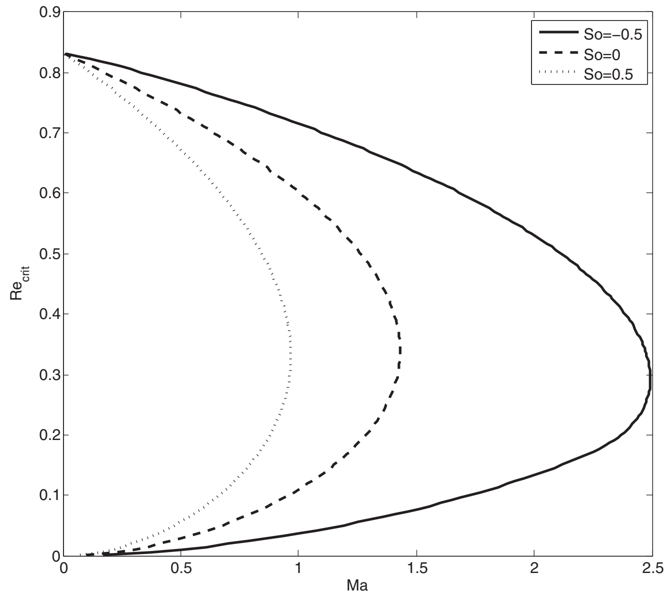

FIG. 5. $\mathrm{Re}_{\mathrm{crit}}$ vs Ma for various So values with Pr $= 7$, Ka $= 100$, Bi $= 1$, $\alpha_T = \alpha_C = 0$, Sc $= 700$, and $\cot\beta = 1$.

Figure 5 contains $\mathrm{Re}_{\mathrm{crit}}$ versus Ma curves for various values of the Soret number for the case with a constant fluid density. The destabilizing effect of increasing So is evident as the region of instability shrinks. This behavior is consistent with the findings of Hu *et al.* [24]. In terms of the magnitude of the Soret effect, which is measured by the absolute value of the Soret number, the indication is that magnifying the Soret effect destabilizes the flow when So is positive and stabilizes it when So is negative. Now, due to the Soret effect, temperature perturbations induce a mass flux which increases concentration differences thus further accentuating the Marangoni stresses. However, if the Soret number is negative, solute is driven towards warmer regions resulting in a higher concentration at the troughs of surface perturbations than at the crests. Since surface tension increases with concentration, the solutal Marangoni stresses pull fluid from the crests to the troughs and thus play a stabilizing role by diminishing the amplitude of interfacial undulations.

We now examine the effect of a variable density. As pointed out by D'Alessio *et al.* [25], a variable density triggers competing instability mechanisms. Effects on stability are specifically due to changes in the magnitude of the density and changes in its gradient with depth. An increase in density contributes to inertia and thus destabilizes the H mode while stabilizing the S mode. Now, a steeper depth gradient of the density enhances stratification in the liquid layer and leads to greater density differences along the surface if its height varies due to the presence of undulations. The result is a greater momentum variation along the surface which generates impulses creating surges and acting to destabilize the H mode. Depending on the values of the relevant parameters a top-heavy stratification can also exist. As a consequence, the crests of a wavy surface will have larger flow rates thus amplifying the waviness of the surface and contributing to instability.

We begin by considering the effect of the scaled thermal expansion coefficient, α_T. In Fig. 6 we show $\mathrm{Re}_{\mathrm{crit}}$ as a function of Ma for different values of α_T. Here we have suppressed the solutal effects by setting the Soret number to zero. In this case it is clear from Eq. (60) that increasing α_T decreases the density at every point in the equilibrium flow, but the stratification increases with α_T and furthermore it is top heavy. Therefore, we expect that increasing α_T will destabilize the S mode, but strengthen both the stabilizing and destabilizing mechanisms affecting the H mode.

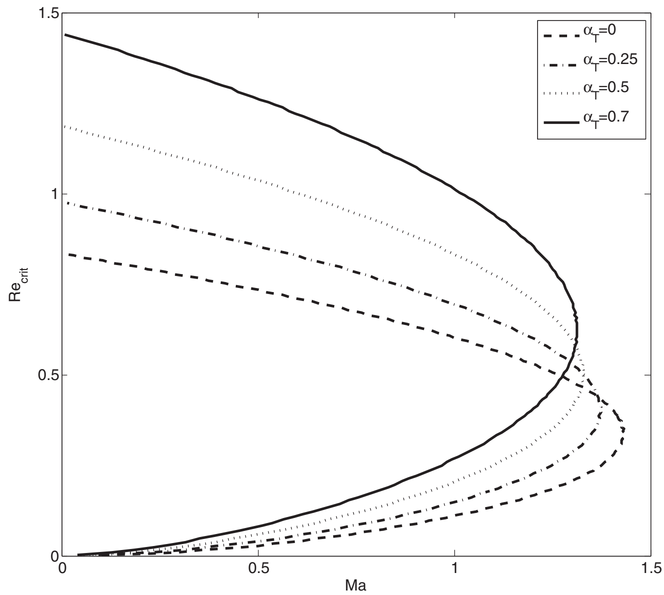

FIG. 6. $\mathrm{Re}_{\mathrm{crit}}$ vs Ma for various α_T values with $\mathrm{Pr} = 7$, $\mathrm{Bi} = 1$, $\mathrm{Ka} = 100$, $\alpha_C = 0$, $\mathrm{So} = 0$, $\mathrm{Sc} = 700$, and $\cot\beta = 1$.

The results in Fig. 6 show that the intervals of unstable Reynolds numbers for the S mode increase with α_T confirming that the S mode is destabilized. It can also be seen that for sufficiently small Marangoni numbers the critical Reynolds number for the onset of the H mode increases with α_T, which indicates that the stabilizing mechanism is dominant. However, for larger values of Ma we see in Fig. 6 that some of the curves cross and the upper branches interchange position indicating that $\mathrm{Re}_{\mathrm{crit}}$ changes from an increasing to a decreasing function of α_T. To better visualize this, in Fig. 7

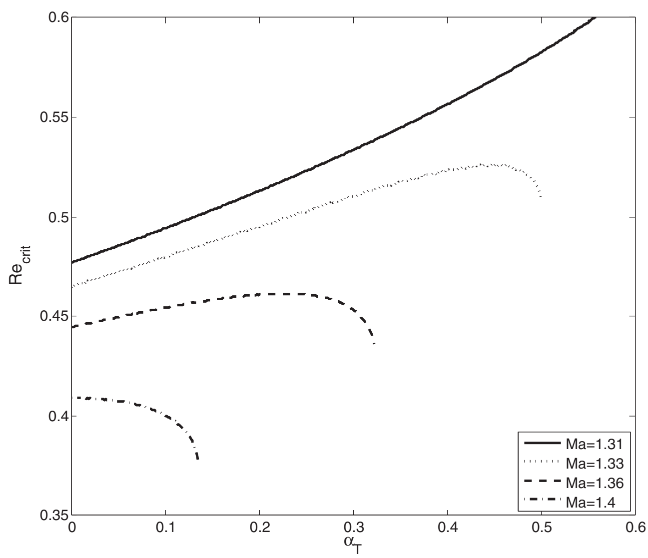

FIG. 7. $\mathrm{Re}_{\mathrm{crit}}$ for the H mode as a function of α_T for various Ma values with $\mathrm{Pr} = 7$, $\mathrm{Bi} = 1$, $\mathrm{Ka} = 100$, $\alpha_C = 0$, $\mathrm{So} = 0$, $\mathrm{Sc} = 700$, and $\cot\beta = 1$.

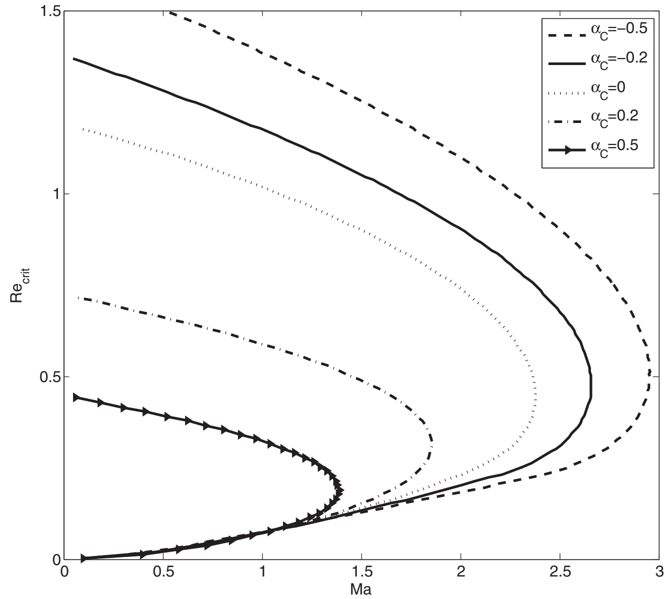

FIG. 8. $\mathrm{Re}_{\mathrm{crit}}$ vs Ma for various α_C values with $\mathrm{Pr} = 7$, $\mathrm{Bi} = 1$, $\mathrm{Ka} = 100$, $\mathrm{So} = -0.5\,\alpha_T = 0.5$, $\mathrm{Sc} = 700$, and $\cot\beta = 1$.

we show $\mathrm{Re}_{\mathrm{crit}}$ for the H mode as a function of α_T for several larger values of Ma taken from Fig. 6. At the right endpoints of the curves in Fig. 7 the critical Reynolds number for the H mode coincides with that for the S mode and the two separate modes are no longer relevant. It can be seen in Fig. 7 that $\mathrm{Re}_{\mathrm{crit}}$ is indeed a decreasing function for certain ranges of α_T, meaning that the destabilizing mechanism associated with density variation now surpasses the stabilizing one. As concluded in Ref. [25], the upshot is that the Marangoni effect couples with the destabilizing mechanism and if sufficiently strong renders it dominant.

One last observation to be drawn from Fig. 6 regarding the effect of increasing α_T is that the lateral extent of the region of stability is shortened. So, if the variation of density with temperature is increased then weaker Marangoni stresses suffice to destabilize the equilibrium flow for all Reynolds numbers.

We now turn to analyzing how variation in density with solutal concentration impacts stability. We find an important correlation between the solutal expansion of the fluid and the Soret effect, which is illustrated in Figs. 8–11. In Figs. 8 and 9 we present $\mathrm{Re}_{\mathrm{crit}}$ as a function of Ma for different values of α_C, with So fixed at a negative value in Fig. 8, while in Fig. 9 So is positive. The results in Fig. 8 indicate that if So is negative, then the critical Reynolds number for the H mode decreases with α_C for all the relevant Marangoni numbers revealing that the H mode is destabilized. In Fig. 9 where So is positive the exact opposite occurs: increasing α_C stabilizes the H mode. We find that, unlike So, the value of α_T does not affect the qualitative effect of varying α_C. This general behavior is explained by considering the equilibrium density given by Eq. (60). The rate of change of the density with respect to α_C is given by $-\mathrm{So}\frac{B}{B+1}z$. Consequently then, if So is negative the density increases with α_C for all values of z. As a result inertial effects are strengthened destabilizing the H mode.

In Figs. 10 and 11 we display $\mathrm{Re}_{\mathrm{crit}}$ as a function of Ma for different values of So. Now, the rate of change of the equilibrium density with respect to So is given by $-\alpha_C\frac{B}{B+1}z$, and thus the density increases or decreases with So depending on the sign of α_C. In Fig. 10 where α_C is negative, the increase in density with So destabilizes the H mode. Figure 10 also reveals that increasing So also destabilizes the S mode, as indicated by an increase with So of the lower branch of the critical

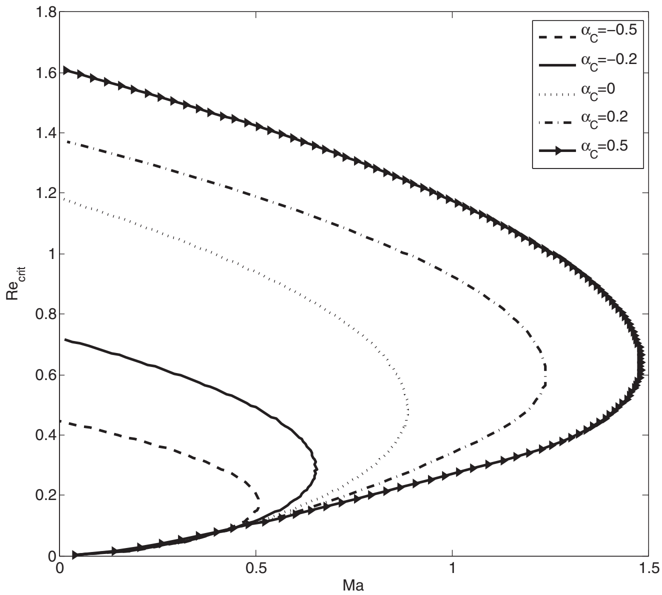

FIG. 9. $\mathrm{Re}_{\mathrm{crit}}$ vs Ma for various α_C values with $\mathrm{Pr} = 7$, $\mathrm{Bi} = 1$, $\mathrm{Ka} = 100$, $\mathrm{So} = 0.5\,\alpha_T = 0.5$,$\mathrm{Sc} = 700$, and $\cot\beta = 1$.

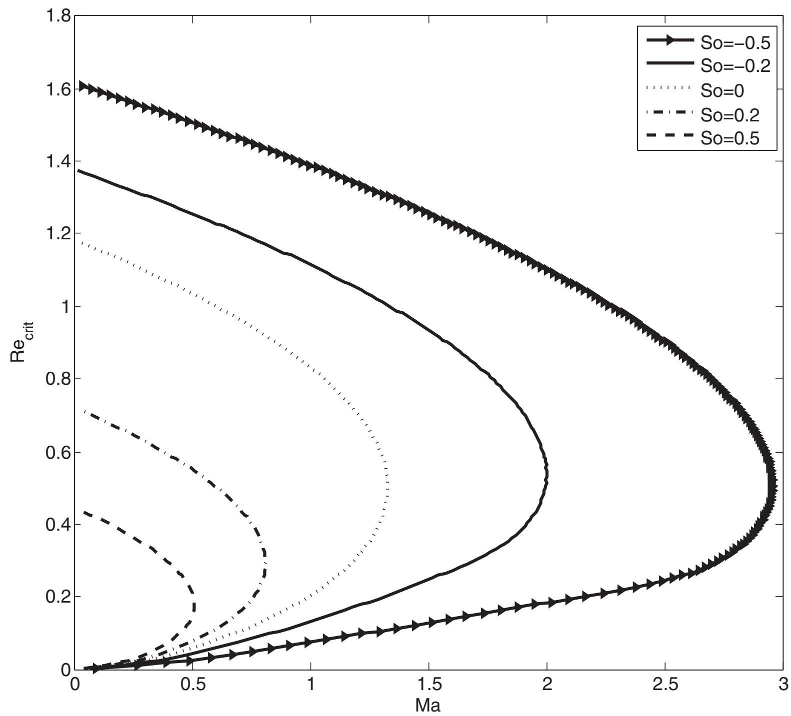

FIG. 10. $\mathrm{Re}_{\mathrm{crit}}$ vs Ma for various So values with $\mathrm{Pr} = 7$, $\mathrm{Bi} = 1$, $\mathrm{Ka} = 100$, $\alpha_C = -0.5\,\alpha_T = 0.5$, $\mathrm{Sc} = 700$, and $\cot\beta = 1$.

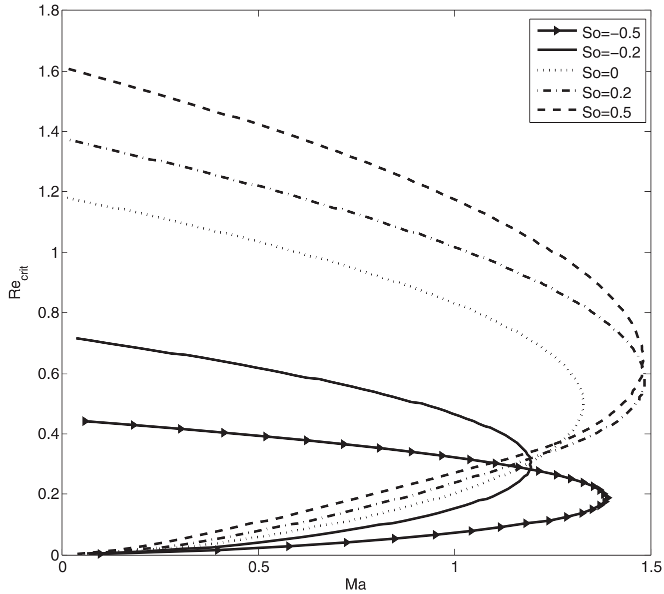

FIG. 11. $\mathrm{Re}_{\mathrm{crit}}$ vs Ma for various So values with $\mathrm{Pr} = 7$, $\mathrm{Bi} = 1$, $\mathrm{Ka} = 100$, $\alpha_C = 0.5\,\alpha_T = 0.5$, $\mathrm{Sc} = 700$, and $\cot\beta = 1$.

Reynolds number curve. As pointed out above, an increase in density has a stabilizing effect on the S mode due to increased inertia. However, the Marangoni stresses are also dependent on the Soret number, and, as it was illustrated in Fig. 5, an increase in So has a destabilizing effect. The results in Fig. 10 suggest that the latter effect is the dominant one, particularly for the larger Marangoni numbers.

We now turn to the case with α_C positive which is exemplified in Fig. 11. In this case density decreases with So, which in itself is a contributor to the stability of the H mode. For Ma values in the small to intermediate range in Fig. 11, $\mathrm{Re}_{\mathrm{crit}}$ on the upper branch of the curve increases with So, and thus the H mode is stabilized. It should be stressed here that for the constant density increasing the Soret number destabilizes the flow, so this behavior is an important consequence of the solutal expansion of the fluid.

Examining the results in Fig. 11 for the larger Marangoni number range, we find that the upper branches of the curves can cross, signaling a reversal of the stabilizing action of the Soret effect akin to the one described above in connection with the thermal expansion effect, as presented in Figs. 6 and 7. The explanation in the present case is that if the Marangoni number is sufficiently large, the coupling of the Soret effect with Marangoni instability surpasses its stabilizing effect related to decreased density and reduced inertia. It is interesting to note that, as is evident in Fig. 10, this phenomenon is not observed if α_C is negative.

We next explore the effect of the strength of surface tension on the onset of instability. Now, surface tension dampens surface undulations, but its effect is negligible on long perturbations. Consequently, in cases when long perturbations are most unstable, like the case shown in Fig. 1, strengthening surface tension, accomplished by increasing the Kapitza number Ka, has no impact on the onset of instability. However, in cases like the one exemplified in Figs. 2 and 3, where the onset of instability is due to the amplification of a perturbation of finite wavelength, the critical Reynolds number is dependent on the Kapitza number. This is illustrated in Fig. 12. It is evident herein that increasing Ka widens the region of stability. This is mostly due to the stabilizing of the H mode which is related to the amplification of surface undulations. It is interesting however to note that increasing Ka also has a stabilizing effect on the S mode. This, together with the stabilizing action of

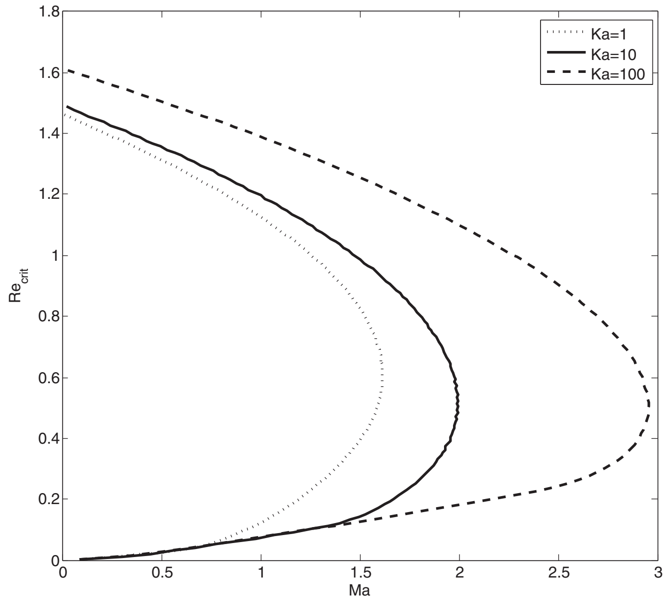

FIG. 12. $\mathrm{Re}_{\mathrm{crit}}$ vs Ma for various Ka values with $\mathrm{Pr} = 7$, $\mathrm{Bi} = 1$, $\alpha_T = 0.5$, $\alpha_C = -0.5$, $\mathrm{So} = -0.5$, $\mathrm{Sc} = 700$, and $\cot\beta = 1$.

the Soret effect for negative So values discussed above in connection with Fig. 5, gives evidence that perturbations in the position of the free surface play a significant role in the instability of the S mode.

V. CONCLUSIONS

In this paper we studied the stability of the flow of a binary liquid film with a deformable surface down a heated incline. The Soret effect was taken into account, whereby the heating induces a mass flux and thus generates concentration differences in the liquid mixture. As in previous studies, surface tension was assumed to decrease with temperature and increase with concentration generating Marangoni stresses. In addition we also considered a variable density for the fluid with the thermal and solutal expansion coefficients as parameters. We assumed the fluid to expand with heating and thus considered only nonnegative values for α_T, but for the solutal expansion coefficient we considered both negative and nonnegative values. Thermal expansion lowers the fluid density but magnifies the stratification in the equilibrium flow. For small Reynolds numbers where inertia is insufficient to amplify surface perturbations, the source of instability is the S mode due to fluid motion along the surface caused by Marangoni stresses. Under these conditions, our linear stability analysis indicates that thermal expansion is a destabilizing factor since the lower density facilitates flow along the surface. For larger Reynolds numbers inertia acts to amplify surface perturbations thus destabilizing the H mode. In this case the decrease in density is a stabilizing factor, however the enhanced stratification has the opposite effect due to the creation of flow rate variations which amplify surface undulations. Our results indicate that for small Marangoni numbers, i.e., when surface tension variations are weak, an increase in the thermal expansion rate stabilizes the H mode. On the other hand, if the Marangoni number is sufficiently large, an increase in thermal expansion destabilizes the equilibrium flow. With regard to the solutal dependence of the density, we found a strong coupling with the Soret effect. An important indicator of the qualitative aspects of flow instability turns out to be the sign of the product of the solutal expansion coefficient and the Soret number, $\alpha_C\mathrm{So}$, and how it affects the variation of the equilibrium density. For example, the solutal expansion of the fluid can stabilize or destabilize the flow depending on the sign of the Soret number.

Similarly, the sign of α_C determines the stabilizing role played by the Soret effect. In particular, if the solutal expansion is positive, then, in contrast to the constant density case, increasing the Soret number stabilizes the flow as long as the Marangoni number is not too large. Another important conclusion resulting from the present study is the coupled effect of solutal expansion and the Soret phenomenon on the shape of the neutral stability curve. Specifically, if the product $\alpha_C\mathrm{So}$ is sufficiently large, then moderately long perturbations are significantly more unstable than infinitely long ones.

ACKNOWLEDGMENT

Financial support for this research was provided by the Natural Sciences and Engineering Research Council of Canada and the Faculty of Mathematics at the University of Waterloo.

APPENDIX

The asymptotic approximation for the critical Reynolds number for small values of the density variation parameters is given by

$$\mathrm{Re}_{\mathrm{crit}} = \frac{10(1+B)^2\cot\beta}{G_1} + F_1\alpha_T + F_2\alpha_C + O\big(\alpha_T\alpha_C,\alpha_T^2,\alpha_C^2\big),$$

where

$$\begin{aligned} G_1 &= 12(1+B)^2 + \frac{5}{16}MB(16+12\mathrm{So}+3\mathrm{So}B),\\ F_1 &= \frac{-2\cot\beta}{7G_1^2}(-3500\,B^4\mathrm{Pr} - 54\,572\,B^4 + 2940\,B^4\mathrm{So}\,M - 13\,000\,B^3\mathrm{Pr} + 18\,445\,B^3\mathrm{So}\,M\\ &\quad - 220\,824\,B^3 + 12\,320\,B^3M - 385\,452\,B^2 + 15\,300\,B^2\mathrm{Pr} + 41\,300\,B^2\mathrm{So}\,M\\ &\quad + 44\,800\,B^2M + 33\,600\,B\mathrm{So}\,M + 24\,800\,B\mathrm{Pr} + 44\,800\,BM - 326\,720\,B - 107\,520), \end{aligned} \tag{A1}$$

$$\begin{aligned} F_2 = \frac{-8\,B\mathrm{So}\cot\beta}{672G_1^2}&(6480\,\mathrm{Sc}\,B^3 - 1\,678\,752\,B^3 + 147\,315\,B^3\mathrm{So}\,M + 5040\,B^3\mathrm{Pr} - 61\,920\,\mathrm{Sc}\,B^2\\ &+ 64\,800\,B^2\mathrm{Pr} - 5\,325\,504\,B^2 + 832\,720\,B^2M + 787\,920\,B^2\mathrm{So}\,M - 143\,280\,\mathrm{Sc}\,B\\ &- 5\,614\,752\,B + 952\,000\,BM + 714\,000\,B\mathrm{So}\,M - 107\,280\,B\mathrm{Pr} - 74\,880\,\mathrm{Sc} - 1\,968\,000\\ &- 167\,040\,\mathrm{Pr}) - \frac{21B\mathrm{So}(3B-4)}{672(B+1)^2\mathrm{Sc}\cot\beta}. \end{aligned} \tag{A2}$$

---

[1] P. L. Kapitza and S. P. Kapitza, Wave flow of thin layers of a viscous fluid, Part III: Experimental study of undulatory flow conditions, Zh. Eksperim. i Teor. Fiz. **19**, 105 (1949).
[2] T. B. Benjamin, Wave formation in laminar flow down an inclined plane, J. Fluid Mech. **2**, 554 (1957).
[3] C.-S. Yih, Stability of liquid flow down an inclined plane, Phys. Fluids **6**, 321 (1963).
[4] R. V. Craster and O. K. Matar, Dynamics and stability of thin liquid films, Rev. Mod. Phys. **81**, 1131 (2009).
[5] S. Kalliadasis, C. Ruyer-Quil, B. Scheid, and M. G. Velarde, *Falling Liquid Films* (Springer, London, 2012).
[6] S. J. D. D'Alessio, J. P. Pascal, and H. A. Jasmine, Instability in gravity-driven flow over uneven surfaces, Phys. Fluids **21**, 062105 (2009).

[7] C. Heining and N. Aksel, Bottom reconstruction in thin-film flow over topography: Steady solution and linear stability, Phys. Fluids **21**, 083605 (2009).

[8] P. M. J. Trevelyan, B. Scheid, C. Ruyer-Quil, and S. Kalliadasis, Heated falling films, J. Fluid Mech. **592**, 295 (2007).

[9] S. J. D. D'Alessio, J. P. Pascal, H. A. Jasmine, and K. A. Ogden, Film flow over heated wavy inclined surfaces, J. Fluid Mech. **665**, 418 (2010).

[10] J. P. Pascal, Linear stability of fluid flow down a porous inclined plane, J. Phys. D **32**, 417 (1999).

[11] T. B. Benjamin, Effects of surface contamination on wave formation in falling liquid films, Arch. Mech. Stosow. **16**, 615 (1964).

[12] S. Whitaker, Effect of surface active agents on the stability of falling liquid films, Ind. Eng. Chem. Fundam. **3**, 132 (1964).

[13] M. G. Blyth and C. Pozrikidis, Effect of surfactant on the stability of film flow down an inclined plane, J. Fluid Mech. **521**, 241 (2004).

[14] A. Pereira, P. M. J. Trevelyan, U. Thiele, and S. Kalliadasis, Dynamics of a horizontal thin liquid film in the presence of reactive surfactants, Phys. Fluids **19**, 112102 (2007).

[15] A. Pereira and S. Kalliadasis, Dynamics of a falling film with solutal Marangoni effect, Phys. Rev. E **78**, 036312 (2008).

[16] G. Karapetsas and V. Bontozoglou, The primary instability of falling films in the presence of soluble surfactants, J. Fluid Mech. **729**, 123 (2013).

[17] G. Karapetsas and V. Bontozoglou, The role of surfactants on the mechanism of long-wave instability in liquid film flows, J. Fluid Mech. **741**, 139 (2014).

[18] J. K. Bhattacharjee, Marangoni convection in binary liquids, Phys. Rev. E **50**, 1198 (1994).

[19] S. W. Joo, Marangoni instabilities in liquid mixtures with Soret effect, J. Fluid Mech. **293**, 127 (1995).

[20] A. Podolny, A. Oron, and A. A. Nepomnyashchy, Long-wave Marangoni instability in a binary-liquid layer with deformable interface in the presence of Soret effect: Linear theory, Phys. Fluids **17**, 104104 (2005).

[21] A. Podolny, A. Oron, and A. A. Nepomnyashchy, Linear and nonlinear theory of long-wave Marangoni instability with the Soret effect at finite Biot numbers, Phys. Fluids **18**, 054104 (2006).

[22] A. Podolny, A. Oron, and A. A. Nepomnyashchy, Long-wave Marangoni instability in a binary liquid layer on a thick solid substrate, Phys. Rev. E **76**, 026309 (2007).

[23] M. Morozov, A. Oron, and A. A. Nepomnyashchy, Nonlinear dynamics of long-wave Marangoni convection in a binary mixture with the Soret effect, Phys. Fluids **25**, 052107 (2013).

[24] J. Hu, H. Ben Hadid, D. Henry, and A. Mojtabi, Linear temporal and spatio-temporal stability analysis of a binary liquid film flowing down an inclined uniformly heated plate, J. Fluid Mech. **599**, 269 (2008).

[25] S. J. D. D'Alessio, C. J. M. P. Seth, and J. P. Pascal, The effects of variable fluid properties on thin film stability, Phys. Fluids **26**, 122105 (2014).

[26] J. Hu, H. Ben Hadid, and D. Henry, Linear stability analysis of Poiseuille-Rayleigh-Bénard flows in binary fluids with Soret effect, Phys. Fluids **19**, 034101 (2007).